Research Square

Preprints are preliminary reports that have not undergone peer review.
They should not be considered conclusive, used to inform clinical practice,
or referenced by the media as validated information.

Numerical Calculation of Vertical Thin-Walled Tanks Filled With Liquid

Elvira Egereva

egerevaen@mail.ru

Moscow State University of Civil Engineering

Andrey Grishin

Atomenergoproekt, JSC

Research Article

Keywords: Thin-walled shell, Cylindrical tank, Membrane theory, Symmetric loading, Python, Finite-difference method, Bending moment, Shear force

Posted Date: June 23rd, 2026

DOI: https://doi.org/10.21203/rs.3.rs-9781534/v1

License: This work is licensed under a Creative Commons Attribution 4.0 International License.
Read Full License

Additional Declarations: No competing interests reported.

NUMERICAL CALCULATION OF VERTICAL THIN-WALLED TANKS FILLED WITH LIQUID

Authors:
Elvira Egereva, Daniil Shlaifer, Andrey Grishin

Affiliations:
Elvira Egereva - PhD in Physical and Mathematical Sciences, Associate Professor, Moscow State University of Civil Engineering, Moscow, Russia (129337, Yaroslavskoye Shosse, 26, Building 2)
Andrey Grishin – PhD in Engineering Sciences, Head of Structural Safety Case Development for Nuclear Facilities, Atomenergoproekt JSC, Moscow, Russia (Moscow, 105005, Bakuniskaya street, 7/1)

Corresponding author: Elvira Egereva
Email: egerevaen@mail.ru

Abstract

The aim of this work is to develop a program for calculating symmetrically loaded thin cylindrical shells filled with fluid. The study presents analytical formulas based on membrane (momentless) theory for computing thin-walled cylindrical shells. A numerical analysis was carried out using a program written in Python employing the finite-difference method. The results obtained for deflections, bending moments, and shear forces were compared to assess the accuracy of the program. It is shown that the numerical error for loaded thin cylindrical shells is minimal. Specifically, the discrepancy between the analytical and software calculations is less than 0.2% for deflection, less than 1.4% for bending moment, and less than 1.6% for shear force. The maximum discrepancy of 1.6% confirms that the software performs calculations for thin-walled cylindrical structures filled with liquid with high accuracy. The discrepancies are attributed to differences in calculation methods, rounding, and finite element size. Despite these minor deviations, the software provides sufficiently accurate results close to manual calculations while simplifying the computation of deflection, bending moment, and shear forces.

Keywords: Thin-walled shell, Cylindrical tank, Membrane theory, Symmetric loading, Python, Finite-difference method, Bending moment, Shear force.

1. Introduction

Calculation of vertical cylindrical thin-walled structures remains relevant in modern times. Cylindrical tanks are used in the oil industry, chemical industry, woodworking, and food industries (including alcohol and dairy sectors), as well as in construction and housing and communal services sectors.

Cylindrical tanks have become widespread due to their ability to have less mass per unit volume compared to non-cylindrical counterparts [1], without compromising strength.

However, errors in tank calculations lead to serious consequences [2]. For example, in February 1979, brittle failure of a vertical cylindrical tank occurred at the Ust-Kuyga oil depot, which had been in operation for less than two years. The accident resulted in the spill of 624 tons of diesel fuel. The cause of brittle failure was the incorrect selection of construction material [3]. This emphasizes the necessity of precise calculations during the design of closed circular cylindrical shells.

It should be noted that in the modern world, most calculations of engineering structures, including vertical cylindrical thin-walled structures, are performed using software complexes. This requires programs to provide results with minimal error. At the same time, it is necessary to achieve minimal discrepancy between numerical calculation results of cylindrical thin-walled structures and software complex calculations.

Solving any statically indeterminate problem in structural mechanics requires consideration from three aspects: geometric, physical, and static. Let us consider one of the simple yet illustrative cases — a cylindrical thin-walled shell. Through this case, we can practically study the nature of errors appearing in calculations performed using software complexes and minimize result deviations.

It is worth noting that the axial symmetry of the cylindrical structure allows converting shear forces and torque to zero.

Recent studies on thin-walled structures interacting with fluids have focused on hydroelastic effects during dynamic loading [24]. Xie et al. [24] experimentally and numerically investigated the oblique impact of an elastic thin-walled structure, demonstrating the complexity of stress responses under asymmetric loading conditions.

2. Materials and Methods

A shell is defined as a body bounded by two curved surfaces, with the distance between them being small compared to other dimensions of the body. Shells belong to continuous solid systems.

A thin-walled shell is characterized by a thickness that is significantly smaller (20 times or more) than other dimensions. The study examines multiple thin-walled cylinders with widths of 4 m and 8 m, thickness of 0.1 m, and height varying from 24 to 192 m.

The shape of the shell's middle surface and its contour determine whether the shell has a closed, open, dome-like, spherical, or cylindrical contour.

When calculating the strength of thin-walled shells, either the "momentless theory" [4] or the more rigorous "moment theory" is applied, depending on various factors.

When analyzing a thin-walled cylindrical shell filled with liquid, calculations are performed using the momentless theory, provided that the tank wall is separated from the bottom.

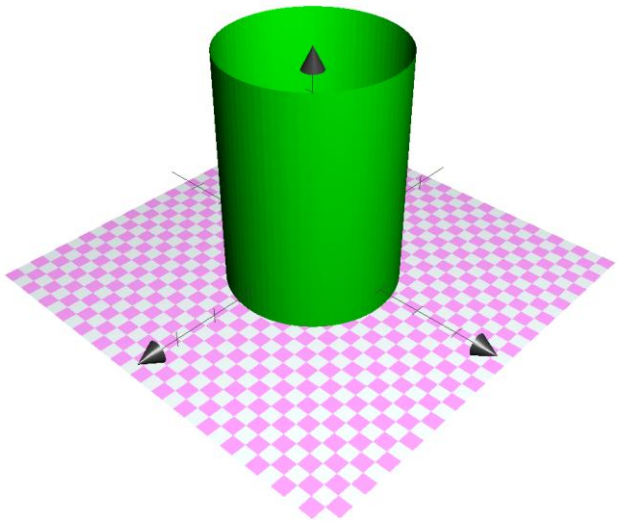


Fig. 1. Three-dimensional visualization of a thin-walled cylindrical shell.

Let us establish a rectangular coordinate system, where the abscissa axis runs along the cylinder's axis of symmetry in the direction of decreasing hydrostatic load, while the ordinate axis lies on the cylinder's bottom plane (the direction is not specified since the abscissa axis serves as the symmetry axis, and the orientation of the ordinate axis will not affect subsequent calculations). The geometry of the structure under consideration is shown in **Figure 1**, which provides a three-dimensional visualization of the thin-walled cylindrical shell employed for the numerical analysis.

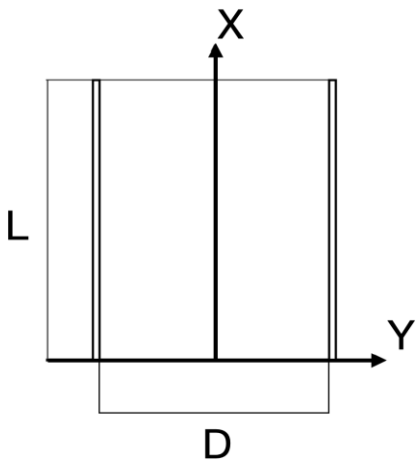


Fig. 2. Visualization of the created coordinate system relative to the vertical section of the cylinder passing through its diameter.

Figure 2 presents a visualization of the created coordinate system relative to the vertical section of the cylinder passing through its diameter. The hydrostatic load function in the specified coordinate system is determined by the formula [5]:

$$p_{\text{restraint}} = \gamma \cdot (L - x), \quad (1)$$

where γ is the specific weight of the liquid filling the cylindrical shell; L is the height of the cylinder**.** The dependence of the hydrostatic restraint pressure on the vertical coordinate (x) is shown in **Figure 3**.

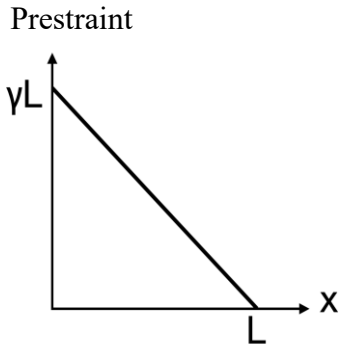


Fig. 3. Graph showing the dependence of hydrostatic restraint pressure ($p_{restraint}$) on the vertical coordinate (x).

Let us determine the hoop stress using the formula:

$$N = p_{\text{restraint}} \cdot R = \gamma \cdot (L - x) \cdot R, \quad (2)$$

where R is the radius of the cylinder. **Figure 4** presents a three-dimensional visualization of the hoop stresses at various points of the cylinder.

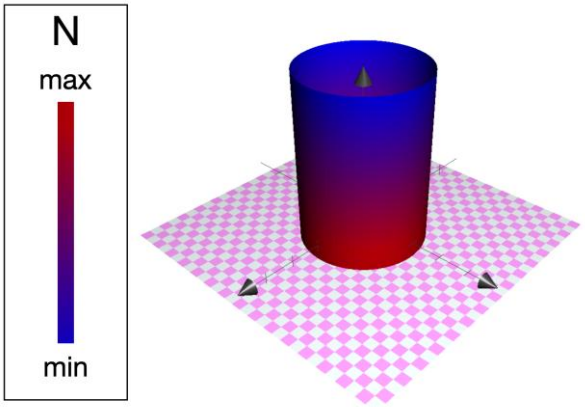


Fig. 4. Three-dimensional visualization of hoop stresses at various points of the cylinder.

Let us calculate the deformations using the formula:

$$\varepsilon = \frac{N}{E \cdot h} = \frac{\gamma \cdot (L - x) \cdot R}{E \cdot h}, \quad (3)$$

where E is the modulus of elasticity of the cylinder material, h is the wall thickness of the cylinder.

Given the axial symmetry of the cylinder and the load acting on it, three equilibrium equations satisfy the identity. The remaining three equations are obtained by projecting all forces onto the X and Y axes and equating to zero the sum of moments of all forces relative to the Y axis. Thus, we obtain a system of three equations for each grid point [6,7]:

$$\begin{cases} \dfrac{dN}{dx} = 0 & (4.1) \\ \dfrac{dQ}{dx} - \dfrac{N}{R} = -p_{\text{restraint}} & (4.2) \\ \dfrac{dM}{dx} - Q = 0 & (4.3) \end{cases} \quad (4)$$

where Q is the shear forces.

Equation (1) can be transformed as follows:

$$\frac{d^2M}{dx^2} - \frac{N}{R} = -p_{\text{restraint}} \tag{5}$$

$$N = E \cdot h \cdot \frac{\omega}{R} \tag{6}$$

$$M = -D \cdot \frac{d^2\omega}{dx^2} \tag{7}$$

$$D \cdot \frac{d^4\omega}{dx^4} + E \cdot h \cdot \frac{\omega}{R^2} = p_{\text{restraint}} \tag{8}$$

The general solution of the non-homogeneous differential equation (8) is represented as the sum of solutions of the corresponding homogeneous differential equation (9):

$$D \cdot \frac{d^4\omega}{dx^4} + E \cdot h \cdot \frac{\omega}{R^2} = 0 \tag{9}$$

and any particular solution of the non-homogeneous differential equation (8), then:

$$\omega = \omega_0 + \omega_1, \tag{10}$$

where

$$\omega_0 = e^{\beta x}\,(\mathrm{D}_1 e^{l\beta x} + \mathrm{D}_2 e^{-l\beta x}) + e^{-\beta l x}\,(\mathrm{D}_3 e^{l\beta x} + \mathrm{D}_4 e^{-l\beta x})\,,$$

It follows that:

$$\omega_0 = e^{\beta x} \cdot \big(D_1 \cdot \cos(\beta x) + D_2 \cdot sin(\beta x)\big) + e^{-\beta x}\big(D_3 \cdot cos(\beta x) + D_4 \cdot sin(\beta x)\big) \tag{11}$$

The particular solution ω_1, which has the form (12):

$$\omega_1 = \gamma \cdot R^2 \cdot \frac{L - x}{E \cdot h} \tag{12}$$

satisfies the inhomogeneous differential equation (13).

Thus, the general solution of the inhomogeneous fourth-order differential equation (9) has the form (13):

$$\omega = e^{\beta x}\big(D_1 cos(\beta x) + D_2 sin(\beta x)\big) + e^{-\beta x}\big(D_3 cos(\beta x) + D_4 sin(\beta x)\big) + \gamma \cdot R^2 \frac{L - x}{E \cdot h} \tag{13}$$

Let us determine the coefficients using the following formulas [8, 9]:

$$\beta = (R \cdot h)^{-\frac{1}{2}} \cdot \left(3 \cdot (1 - \nu^2)\right)^{\frac{1}{4}}, \quad (14)$$

$$D_3 = -R^2 \cdot \gamma \cdot \frac{L}{E \cdot h}, \quad (15)$$

$$D_4 = R^2 \cdot \frac{\gamma \cdot (1 - \beta \cdot L)}{E \cdot h \cdot \beta}, \quad (16)$$

Then the deflection ω(x) is determined by the formula (17) [10, 11]:

$$\omega(x) = e^{-\beta x}\left(D_3 cos(\beta x) + D_4 sin(\beta x)\right) + \gamma \cdot R^2 \cdot \frac{L - x}{E \cdot h} \quad (17)$$

The bending moment M(x) and shear forces Q(x) are determined by the following formulas (18) and (19) [12, 13]:

$$M(x) = -D \cdot \omega''(x), \quad (18)$$

$$Q(x) = -D \cdot \omega'''(x), \quad (19)$$

where the cylindrical rigidity is determined by the formula (20) [14]:

$$D = E \cdot \frac{h^3}{12 \cdot (1 - \nu^2)} \quad (20)$$

where ν is the Poisson's ratio.

To determine the numerical values of deformation, bending moment, and shear force, Program No. 1 was developed in the Python programming language. The program utilizes the finite difference method [15-17] and incorporates the math and matplotlib libraries.

The process begins by defining variables (**Figure 5**). The float(input()) functions are used to accept input values as floating-point numbers, which enable working with fractions and performing arithmetic operations with high precision. This input function is repeated to determine all necessary values: cylinder height (L), cylinder radius (R), wall thickness (h), Poisson's ratio (ν), elastic modulus (E), and fluid specific weight (γ).

The use of floating-point numbers ensures accurate calculations required for engineering analysis of cylindrical structures [18, 19].

```
import math
import matplotlib.pyplot as plt
L=float(input("Высота цилиндра [м]: "))
R=float(input("Радиус цилиндра [м]: "))
h=float(input("Толщина стенки цилиндра [м]: "))
v=float(input("Коэффициент Пуассона: "))
E=float(input("Модуль упругости [10^8 * кН/м^2]: "))*(10**8)
y=float(input("Удельный вес жидкости [кН/м^3]: "))
```

Fig. 5. Demonstration of the code section responsible for defining variables: cylinder height (L), cylinder radius (R), wall thickness (h), elastic modulus (E), specific weight of the liquid (γ) and constants – Poisson's ratio (ν).

At the next step (**Figure 6**), Program No. 1 provides all necessary constants for calculations: bet (β), D3 (D3), D4 (D4), which are calculated using formulas (7.1) - (7.3). Additionally, the program computes the cylindrical rigidity (D) values based on formula (11). The deflection is calculated by calling the function ω(x).

```
D=(E*h**3)/(12*(1-v**2))
bet=((1/(R*h))**(1/2))*(3*(1-v**2))**(1/4)
D3=(-(R**2)*y*L/E/h)
D4=(R**2)*y*(1-bet*L)/E/h/bet
lam=math.pi/bet
print(E*h/R)
print(D)

def w(x):
    global bet, D3, D4, R, E, h, y
    return math.exp(-bet*x)*(D3*math.cos(bet*x)+D4*math.sin(bet*x))+(R**2*(y*(L-x)))/(E*h)
```

Fig. 6. Demonstration of the code section responsible for calculating: cylindrical rigidity (D) and coefficients bet (β), D3 (D3), D4 (D4) defining the deflection function (ω(x)).

The functions m(x) and q(x) determine the bending moment and shear forces at point x using the finite difference method.

```
def m(x):
    global D
    dx = 0
    w11 = (w(x + 1 / (dx)) - w(x)) * (dx)
    w12 = (w(x + 2 / (dx)) - w(x + 1 / (dx))) * (dx)
    w2 = (w12 - w11) * (dx)
    return -D * w2


def q(x):
    global D
    dx = 0
    w11 = (w(x + 1 / (dx)) - w(x)) * (dx)
    w12 = (w(x + 2 / (dx)) - w(x + 1 / (dx))) * (dx)
    w13 = (w(x + 3 / (dx)) - w(x + 2 / (dx))) * (dx)
    w21 = (w12 - w11) * (dx)
    w22 = (w13 - w12) * (dx)
    w31 = (w22 - w21) * (dx)
    return -D * w31
```

Fig. 7. Demonstration of the code section responsible for defining the functions of bending moment (m(x)) and shear forces (q(x)). The difference that will provide optimal values has not been determined yet; it is recorded as the variable dx.

Figure 7 shows the section of code responsible for defining the functions of the bending moment (m(x)) and shear forces (q(x)). The difference that will provide optimal values has not been determined yet and is recorded as the variable dx. In Python, variables do not store the value itself, but rather a reference to that value in the computer's memory. These values are limited and do not have infinite precision. This means that the more digits a number has and the more operations are performed on it, the greater the discrepancy between the actual result and the result produced by Python.

That is why it is important to avoid using extremely small values of Δx when applying the finite difference method in Python [18, 19].

$$f'(x_0) = \frac{f(x_0 + \Delta x) - f(x_0)}{\Delta x} \quad \text{when } \Delta x \to 0, \tag{21}$$

At the same time, the derivative is the limiting value of the rate of change of a function as the change in the argument approaches zero (18). The smaller the increment of the argument, the more accurately one can approach the correct value of the derivative [20, 21, 23].

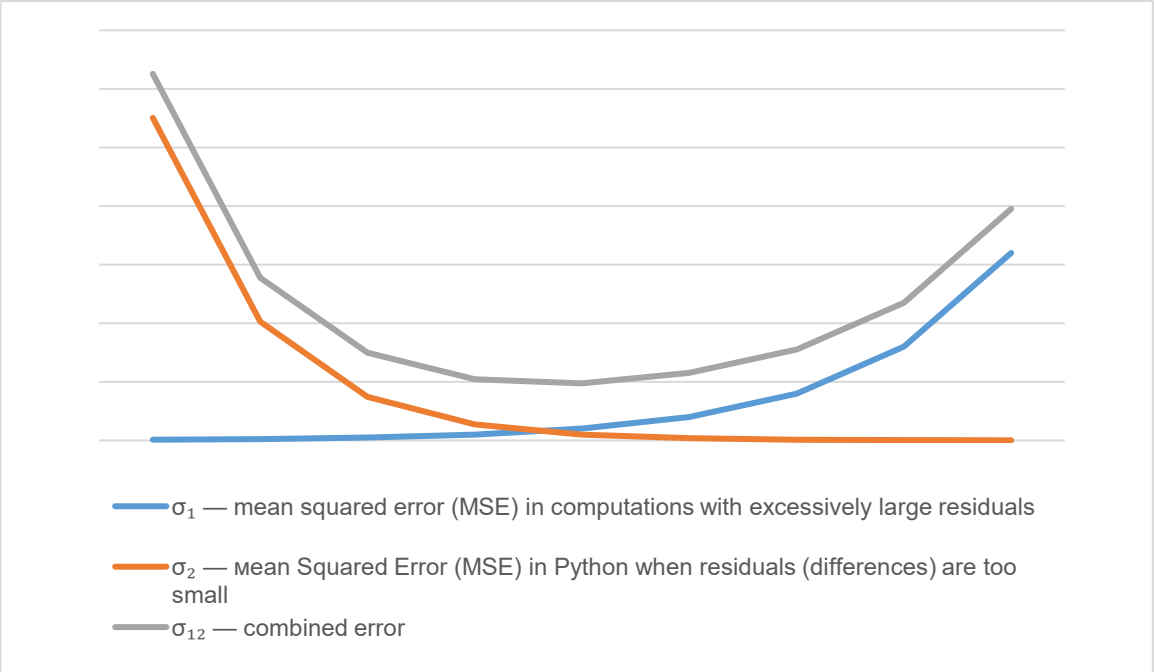


Fig. 8. Schematic graph showing the dependence of the root mean square deviation on the number of decimal places in the number used as the difference step in the finite difference method within a Python-based software package.

Figure 8 presents a schematic graph showing the dependence of the root mean square deviation on the number of decimal places in the number used as the difference step in the finite difference method. It is necessary to determine the optimal value of Δx that will produce the smallest resulting error in Program No. 1. For this purpose, Program No. 2 is created, whose operating principle involves comparing the already found numerical values of the bending moment M(x) and transverse forces Q(x) with the result provided by the program at different values of the step Δx (**Figure 9**).

Program No. 2 calculates the root-mean-square deviation of Q(x) and M(x) for various changes in the argument. To optimize the iteration of Δx in Program No. 2, the following is adopted: 〖Δx = 2〗^((-n)/A), where n is a variable value, and A is the inverse of the iteration step Δx.

This method is as efficient as iterating through all options because computers store data in a binary number system. This makes it clear that storing all numbers from 2^(1-n) to 2^(-n) will occupy the same amount of computer memory and provide the same error for the same calculations.

If all numbers in the range provide the same error in Program No. 2 calculations, the one closest to 0 is selected (since the derivative is the rate of change of the function as the change in the argument approaches zero). In this case, the number closest to zero is 2^(-n).

```
for z in range(3, 16):
    L=12*(0.1*(2**(z/3)))
    sver=3.82*(0.1*(2**(z/3)))
    poperF = 0
    min = 100
    min_pos = 0
    for delta in range(1, 17 * 4):
        delx = 2 ** (delta / 4)
        for x in range(int(L) * 2000):
            if poperF >= q(x / 2000, delx):
                poperF = q(x / 2000, delx)
        Oy.append((poperF + 3.82) ** 2)
        Ox.append(delta / 4)

        if (poperF + 3.82) ** 2 <= min:
            min = (poperF + 3.82) ** 2
            min_pos = delta
    print()
    print(min_pos)
    print(min)
```

Fig. 9. Double loop verifying the discrepancy between the true and calculated values, running 13 times with previously calculated transverse forces of cylinders.

Program Output Result:

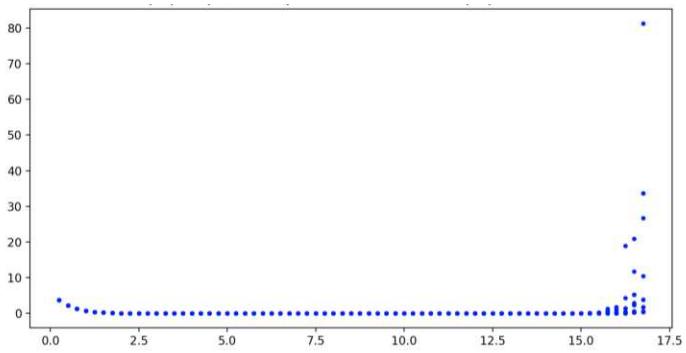


Fig. 10. Graph of 13 discrete functions showing the deviation of the calculated Q(x) from the actual value at different Δx values.

Figure 10 presents a graph of 13 discrete functions showing the deviation of the calculated value of Q(x) from the actual value at different Δx values. The smallest error was observed in all 13 experiments with step A = 4 at n = 14. Consequently, in the finite difference method, we will adopt:

$$\Delta x = 2^{-14/4} = 2^{-3.5} = 0{,}08838834765...$$

These values are used in Program No. 1, which provides numerical values for deflection, bending moment, and transverse forces (**Figure 11**).

```
def q(x):
    global D
    dx = 2**(7/2)
    w11 = (w(x + 1 / (dx)) - w(x)) * (dx)
    w12 = (w(x + 2 / (dx)) - w(x + 1 / (dx))) * (dx)
    w13 = (w(x + 3 / (dx)) - w(x + 2 / (dx))) * (dx)
    w21 = (w12 - w11) * (dx)
    w22 = (w13 - w12) * (dx)
    w31 = (w22-w21)*(dx)
    return -D*w31
```

Fig. 11. Function q(x) considering the new dx value.

Program No. 2 uses a for loop to analyze the cylinder from its bottom point to its top point with a step of 0.5 mm. By repeatedly calling the functions ω(x), M(x), and Q(x), we obtain a uniform graph of bending, bending moment, and transverse forces for a thin-walled cylinder. Additionally, this process provides the maximum values of these functions on the interval [0, L], where L is the height of the cylinder.

```
progib = 0
Ox = []
Oy = []
Oy1 = []
Oy2 = []
for x in range(int(L) * 2000):
    if progib <= w(x / 2000):
        progib = w(x / 2000)
    if x % 5 == 0:
        Oy.append(w(x / 2000))
        Ox.append(x / 2000)
print("Максимальный прогиб [мм]: ", progib * 1000)

izgmom = 0
for x in range(int(L) * 2000):
    if izgmom <= m(x / 2000):
        izgmom = m(x / 2000)
    if x % 5 == 0:
        Oy1.append(m(x / 2000))
print('Изгибающий момент [кНм]: ', izgmom)
poperF = 0
for x in range(int(L) * 2000):
    if poperF >= q(x / 2000):
        poperF = q(x / 2000)
    if x % 5 == 0:
        Oy2.append(q(x / 2000))
print('Поперечные силы [кН]: ', -poperF)
```

Fig. 12. Program section analyzing functions ω(x), q(x), m(x) on the interval [0, L] with a step of 0.5 mm.

Figure 12 shows the program section that analyzes the functions ω(x), q(x), m(x) on the interval [0, L] with a step of 0.5 mm. At the end of the program, three graphs are generated showing the dependence of functions ω(x), M(x), and q(x) on the argument x. The console outputs the maximum function values within the domain.

The following tasks are solved using the program method. Initial data for three tasks are set:

1. Cylinder height: L = 12 [m]; Cylinder radius: R = 4 [m]; Wall thickness: h = 0.1 [m]. The constructed dependence curves, as well as maximum function values, are shown in **Figure 13–14**.
2. Cylinder height: L = 24 [m]; Cylinder radius: R = 8 [m]; Wall thickness: h = 0.1 [m]. The constructed dependence curves, as well as maximum function values, are shown in **Figure 15–16**.
3. Cylinder height: L = 24 [m]; Cylinder radius: R = 4 [m]; Wall thickness: h = 0.1 [m]. The constructed dependence curves, as well as maximum function values, are shown in **Figure 17–18**.

All three tasks use the following values: poisson's ratio: ν = 0.24, elastic modulus: $E = 2 \times 10^8$ [kN/m²], specific weight of liquid: γ = 9.81 [kN/m³].

This approach allows for a comprehensive analysis of cylinder behavior under different geometric parameters while maintaining consistent material properties and loading conditions [22].

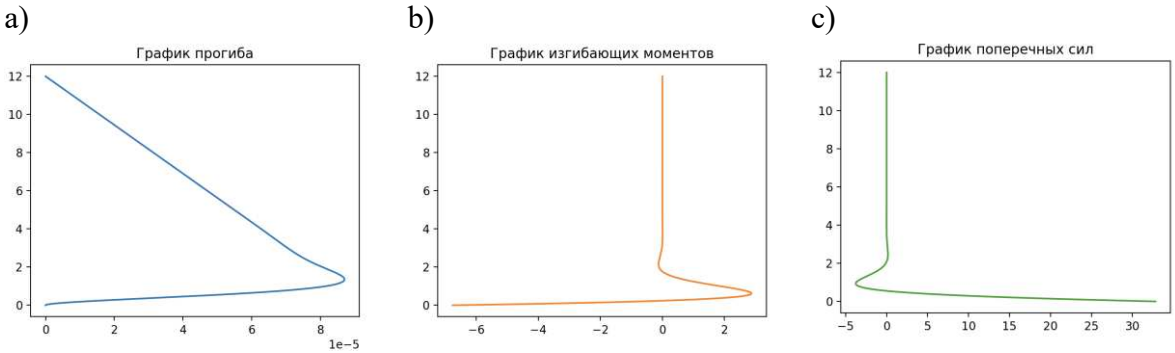


Fig. 13. Calculation results from the software complex: graphs of deflection (a), bending moment (b), and transverse forces (c) for the first task.

```
Высота цилиндра [м]: 12
Радиус цилиндра [м]: 4
Толщина стенки цилиндра [м]: 0.1
Коэффициент Пуассона: 0.24
Модуль упругости [10^8 * кН/м^2]: 2
Удельный вес жидкости [кН/м^3]: 9.81
Максимальный прогиб [мм]:  0.08701655603454543
Изгибающий момент [кНм]:  2.8707640009216546
Поперечные силы [кН]:  3.7681414348657127
```

Fig. 14. Maximum values of deflection, bending moment, and transverse force functions for the first task.

a) b) c)

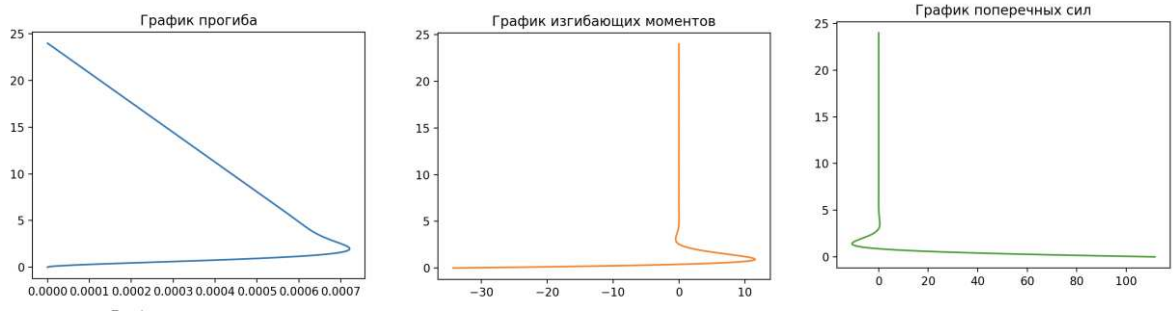


Fig. 15. Calculation results from the software complex: deflection graphs (a), bending moment (b), and transverse forces (c) for the second task.

```
Высота цилиндра [м]: 24
Радиус цилиндра [м]: 8
Толщина стенки цилиндра [м]: 0.1
Коэффициент Пуассона: 0.24
Модуль упругости [10^8 * кН/м^2]: 2
Удельный вес жидкости [кН/м^3]: 9.81
Максимальный прогиб [мм]:  0.7212845481863521
Изгибающий момент [кНм]:  11.56279165451562
Поперечные силы [кН]:  10.770266545364208
```

Fig. 16. Maximum values of deflection, bending moment, and transverse force functions for the second task.

a) b) c)

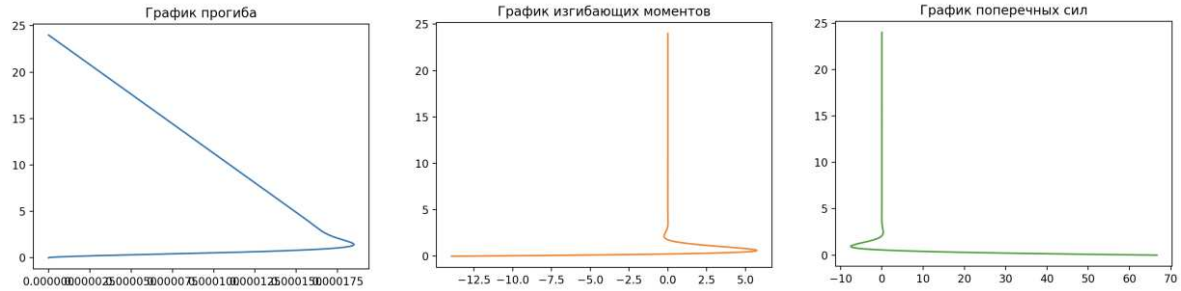


Fig. 17. Calculation results from the software complex: deflection graphs (a), bending moment (b), and transverse forces (c) for the first task.

```
Высота цилиндра [м]: 24
Радиус цилиндра [м]: 4
Толщина стенки цилиндра [м]: 0.1
Коэффициент Пуассона: 0.24
Модуль упругости [10^8 * кН/м^2]: 2
Удельный вес жидкости [кН/м^3]: 9.81
Максимальный прогиб [мм]:  0.18490085867625208
Изгибающий момент [кНм]:  5.739691728076276
Поперечные силы [кН]:  7.53387501871894
```

Fig. 18. Maximum values of deflection, bending moment, and transverse force functions for the first task.

To verify the correctness of the results, a calculation of similar problems is performed using the analytical method - utilizing the previously obtained formulas for deflection, bending moment, and transverse forces (17), (18), (19):

$$\omega = e^{-\beta x}(D_3\cos(\beta x) + D_4\sin(\beta x)) + \gamma \cdot R^2(L - x)/(E \cdot h),$$

$$M(x) = -D \cdot \omega''(x), \tag{22}$$

$$Q(x) = -D \cdot \omega'''(x), \tag{23}$$

As well as the formulas for coefficients (14), (15), (16), (20).

For the first task: $\beta = 2.05$ [m^{-1}], $D_3 = -9.4 \cdot 10^{-5}$ [m], $D_4 = -9.03 \cdot 10^{-5}$ [m], $D = 17685$ [kN·m].

For the second task: $\beta = 1.45$ [m^{-1}], $D_3 = -7.5 \cdot 10^{-4}$ [m], $D_4 = -3.7 \cdot 10^{-4}$ [m], $D = 17685$ [kN·m].

For the third task: $\beta = 1.45$ [m^{-1}], $D_3 = -3.8 \cdot 10^{-4}$ [m], $D_4 = -2.6 \cdot 10^{-4}$ [m], $D = 17685$ [kN·m].

The calculation results are obtained using the PTC Mathcad Prime software package.

For the first task: maximum deflection ω = 0.087 [mm], maximum bending moment M = 2.91 [kN·m], maximum shear forces Q = 3.82 [kN].

For the second task: maximum deflection ω = 0.72 [mm], maximum bending moment M = 11.64 [kN·m], maximum shear forces Q = 10.8 [kN].

For the third task: maximum deflection ω = 0.185 [mm], maximum bending moment M = 11.64 [kN·m], maximum shear forces Q = 10.8 [kN].

3. Results

Table 1. Comparison of analytical and software calculation results with elastic modulus E = $2 \cdot 10^8$ [kN/m²], fluid specific weight γ = 9.81 [kN/m³], Poisson's ratio ν = 0.24.

	Cylinder height [m]	Cylinder radius [m]	Wall thickness [m]	Deflection [mm]	Bending moment [kN·m]	Shear force [kN]
Software calculation	12	4	0.1	0.08701	2.8707	3.7681
Analytical calculation				0.087	2.91	3.82
Software calculation	24	8	0.1	0.7212	11.5628	10.7702
Analytical calculation				0.72	11.64	10.8
Software calculation	24	4	0.1	0.1849	5.7396	7.5338
Analytical calculation				0.185	5.82	7.64
Discrepancy between analytical and software calculation results				<0,2%	<1,4%	<1,6%

To verify the accuracy of the software model, a comparison was performed with the analytical solution. As shown in **Table 1**, the discrepancy between the results does not exceed 1,6% for the shear force and is less than 0,2% for the deflection. This confirms the adequacy of the developed software model for further calculations.

4. Conclusions

1. The observed pressure oscillations in the present study are consistent with those reported by Xie et al. [24] for elastic thin-walled structures under dynamic fluid loading, where wavelet analysis revealed multiple frequency components associated with hydroelastic coupling.
2. The discrepancy between the analytical and software calculation results is less than 0,2% for deflection, less than 1,4% for bending moment, and less than 1,6% for shear force.
3. The maximum discrepancy of 1,6% indicates that the software performs calculations for thin-walled cylindrical structures filled with liquid with high accuracy.
4. The discrepancies are caused by differences in calculation methods, rounding, and the size of finite elements. Despite these discrepancies, the software provides sufficiently accurate results close to manual calculations while simplifying the computation of deflection, bending moment, and shear forces.
5. For practical applications, it is recommended to take bending moment and shear force values 2% higher and deflection 0,5% higher than those provided by the software to compensate for the maximum discrepancy in the lower direction.

Declarations

Ethics approval and consent to participate

Not applicable.

Consent for publication

Applicable.

Availability of data and material

Data and material will be provided upon request if necessary.

Competing interests

The authors declare that they have no competing interests

Funding

Not applicable.

Authors' contributions

The authors equally contributed to the present research at all stages from the formulation of the problem to the final findings and solution.

Acknowledgements

Not applicable.

5. References

1. Paimushin V.N. (2007) Problems of geometric non-linearity and stability in the mechanics of thin shells and rectilinear columns. Journal of Applied Mathematics and Mechanics 71(5):772-805. https://doi.org/10.1016/j.jappmathmech.2007.11.012
2. Park J., Han S., Park C., Kim T. (2025) Investigation of verticality criteria on aboveground oil storage tanks. KSCE Journal of Civil Engineering (100449):2–36. https://doi.org/10.1016/j.kscej.2025.100449
3. Andreev Y.M. (2017) Obespechenie ekspluatacionnoy nadezhnosti rezervuarov severa putem povysheniya vyyavlyaemosti ploskostnyh defektov [Ensuring the operational reliability of northern tanks by increasing the detectability of planar defects]. Abstract of Cand Sci (Tech) Dissertation. Yakutsk. https://www.hydro.nsc.ru/docs/Diss/AndreevDissertation.pdf
4. Burlakova A.M., Kondratyeva L.E., Mavrina S.A., Filatov V.V. (2017) Mathematical modeling. Vladimir State University, Vladimir, 18 p.
5. Kemalov A.F., Sultanov V.A., Milyutina V.A., Karataev O.R. (2024) Fundamentals of fluid and gas mechanics. Hydrostatics. Hydrodynamics. Kazan University Press, Kazan

6. Sachenkov A.A. (2018) Tsikl lektsiy po teorii plastin i obolochek [Cycle of lectures on the theory of plates and shells]. Kazan University, Kazan.
7. Gredasova N.V., Andreeva I.Y. (2022) Obyknovennye differentsial'nye uravneniya [Ordinary differential equations]. Ural University Press. https://elar.urfu.ru/handle/10995/119772
8. Al Malul R., Stupivtsev A. (2022) Asimmetrichno nagruzhennye zamknutye krugovye tsilindricheskie obolochki [Asymmetrically loaded closed circular cylindrical shells]. BST: Bulletin of Construction Technology (1050):38–41
9. Egereva E.N., Egerev A.Y., Zubov A.O. (2018) Poperechnye kolebatel'nye dvizheniya v vyazkoy zhidkosti, kontaktiruyushchey s poristoy sredoy [Transverse oscillatory motions in a viscous fluid in contact with a porous medium]. Vestnik Mordovskogo Universiteta 28(2):164–174. https://doi.org/10.15507/0236-2910.028.201802.164-174
10. Egereva E.N., Barmenkov A.S.(2019) Overload in the roof trusses of the Media Center building in Saransk. E3S Web of Conferences 110:01079. https://doi.org/10.1051/e3sconf/201911001079
11. Aleksandrov A.V., Potapov V.D. (2002) Soprotivlenie materialov. Osnovy teorii uprugosti i plastichnosti [Strength of materials. Fundamentals of the theory of elasticity and plasticity]. Vysshaya shkola, Moscow
12. Annin B.D., Volchkov Y.M. (2016) Neklassicheskie modeli teorii plastin i obolochek [Non-classical models of the theory of plates and shells]. Journal of Applied Mechanics and Technical Physics 57(5):5–14. https://doi.org/10.15372/PMTF20160501
13. Dobronravov V.V., Nikitin N.N. (1983) Kurs teoreticheskoy mekhaniki [Course of theoretical mechanics]. Vysshaya shkola, Moscow.
14. Zhilin P.A. (2006) Aktual'nye problemy mekhaniki. Sbornik statey po materialam dokladov na ezhegodnoy Mezhdunarodnoy letney shkole-konferentsii «Aktual'nye problemy mekhaniki» [Actual problems of mechanics. Collection of articles based on reports at the annual International Summer School-Conference «Actual Problems of Mechanics»], Vol. 1. Institute of Problems of Mechanical Engineering RAS, Saint Petersburg. https://ipme.ru/ipme/labs/dms/prive/ivanova/Home_page_Elena_Ivanova/PDF/Zhilin_2006_APM_rus.pdf

15. Degtyarev A.A. (2011) Metod konechnyh raznostey [Finite difference method]. Samara State Aerospace University, Samara
16. Dheyaaldin M.H., Özakça M. (2017) Effect of stiffeners on structural behavior of steel liquids tank. International Journal of Engineering and Applied Sciences 2(3)
17. Xi C., Zeng X., Pu M. (2016) Dynamic characteristics and seismic response analysis of vertical cylindrical oil storage tank. Petrochemical Equipment (4)
18. Goudarzi M.A., Sabbagh-Yazdi S.R. (2008) Evaluating 3D earthquake effects on sloshing wave height of liquid storage tanks using finite element method. Journal of Seismology and Earthquake Engineering 10(3)
19. Gonçalves P.B., Ramos NRSS (1996) Free vibration analysis of cylindrical tanks partially filled with liquid. Journal of Sound and Vibration 195(3):429–444.
20. Mazuch T., et al (1996) Natural modes and frequencies of a thin clamped-free steel cylindrical storage tank partially filled with water — FEM and measurement. Journal of Sound and Vibration 193(3):669–690
21. Housner G.W. (1963) The dynamic behavior of water tanks. Bulletin of the Seismological Society of America 53(2):381–387
22. Burke J.E. (2008) Discrete models for seismic analysis of liquid storage tanks of arbitrary shape and fill height. Journal of Pressure Vessel Technology 130(4)
23. Liu N., Zhou X., Ma H., Chen G., Zhang M., Zuo Z., Ren H. (2026) Experimental and numerical study on the slamming pressure characteristics of a thin-walled air cushion with flexible skirts. Ocean Engineering 351(Part 1):124330. https://doi.org/10.1016/j.oceaneng.2026.124330
24. Xie H. et al. (2024) Hydroelastic analysis of an elastic thin-walled structure obliquely impacting a calm water surface. Thin-Walled Structures 197:111638. https://doi.org/10.1016/j.tws.2024.111638